

# Evidence for the two pole structure of the $\Lambda(1405)$ resonance

V.K. Magas<sup>1</sup>, E. Oset<sup>1</sup>, A. Ramos<sup>2</sup>

<sup>1</sup> *Departamento de Física Teórica and IFIC, Centro Mixto,  
Institutos de Investigación de Paterna - Universidad de Valencia-CSIC  
Apdo. correos 22085, 46071, Valencia, Spain*

<sup>2</sup> *Departament d'Estructura i Constituents de la Matèria,  
Universitat de Barcelona,  
Diagonal 647, 08028 Barcelona, Spain*

The  $K^-p \rightarrow \pi^0\pi^0\Sigma^0$  reaction is studied within a chiral unitary model. The distribution of  $\pi^0\Sigma^0$  states forming the  $\Lambda(1405)$  shows, in agreement with a recent experiment, a peak at 1420 MeV and a relatively narrow width of  $\Gamma = 38$  MeV. The mechanism for the reaction is largely dominated by the emission of a  $\pi^0$  prior to the  $K^-p$  interaction leading to the  $\Lambda(1405)$ . This ensures the coupling of the  $\Lambda(1405)$  to the  $K^-p$  channel, thus maximizing the contribution of the second state found in chiral unitary theories, which is narrow and of higher energy than the nominal  $\Lambda(1405)$ . This is unlike the  $\pi^-p \rightarrow K^0\pi\Sigma$  reaction, which gives more weight to the pole at lower energy and with a larger width. The data of these two experiments, together with the present theoretical analysis, provides a firm evidence of the two pole structure of the  $\Lambda(1405)$ .

PACS numbers: 13.75.-n, 12.39.Fe, 14.20.Jn, 11.30.Hv

The history of the  $\Lambda(1405)$  as a dynamical resonance generated from the interaction of meson baryon components in coupled channels is long [1], but it has experienced a boost within the context of unitary extensions of chiral perturbation theory ( $U\chi PT$ ) [2, 3, 4, 5, 6, 7], where the lowest order chiral Lagrangian and unitarity in coupled channels generates the  $\Lambda(1405)$  and leads to good agreement with the  $K^-p$  reactions. The surprise, however, came with the realization that there are two poles in the neighborhood of the  $\Lambda(1405)$  both contributing to the final experimental invariant mass distribution [5, 6, 7, 8, 9, 10, 11]. The properties of these two states are quite different, one has a mass around 1390 MeV, a large width of about 130 MeV and couples mostly to  $\pi\Sigma$ , while the second one has a mass around 1425 MeV, a narrow width of about 30 MeV and couples mostly to  $\bar{K}N$ . The two states are populated with different weights in different reactions and, hence, their superposition can lead to different distribution shapes. Since the  $\Lambda(1405)$  resonance is always seen from the invariant mass of its only strong decay channel, the  $\pi\Sigma$ , hopes to see the second pole are tied to having a reaction where the  $\Lambda(1405)$  is formed from the  $\bar{K}N$  channel. In this sense a calculation of the  $K^-p \rightarrow \gamma\Lambda(1405)$  reaction [12], prior to the knowledge of the existence of the two  $\Lambda(1405)$  poles, showed a narrow structure at about 1420 MeV. With the present perspective this is clearly interpreted as the reaction proceeding through the emission of the photon followed by the generation of the resonance from  $K^-p$ , thus receiving a large contribution from the second narrower state at higher energy. The same idea is used in the reaction  $\gamma p \rightarrow K^*\Lambda(1405)$  [13] which proceeds via K-meson exchange and is now under investigation at Spring8/Osaka [14]. Luckily, the recently measured reaction  $K^-p \rightarrow \pi^0\pi^0\Sigma^0$  [15] allows us to test already the two-pole nature of the  $\Lambda(1405)$ . This process shows a strong similarity with the reaction  $K^-p \rightarrow \gamma\Lambda(1405)$ ,

where the photon is replaced by a  $\pi^0$ .

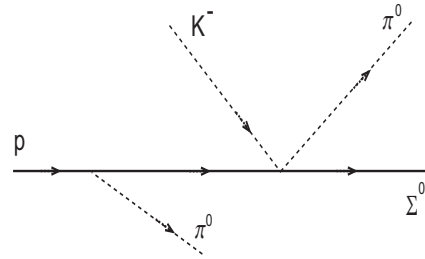


FIG. 1: Nucleon pole term for the  $K^-p \rightarrow \pi^0\pi^0\Sigma^0$  reaction.

Our model for the reaction  $K^-p \rightarrow \pi^0\pi^0\Sigma^0$  in the energy region of  $p_{K^-} = 514$  to 750 MeV/c, as in the experiment [15], considers those mechanisms in which a  $\pi^0$  loses the necessary energy to allow the remaining  $\pi^0\Sigma^0$  pair to be on top of the  $\Lambda(1405)$  resonance. The first of such mechanisms is given by the diagram of Fig. 1. In addition, analogy with the  $\pi^-p \rightarrow K^0\pi\Sigma$  reaction, where the  $\pi\Sigma$  is also produced in the  $\Lambda(1405)$  region, demands that one also considers the mechanisms of Fig. 2. Indeed, the analogous diagrams replacing  $(K^-, \pi^0)$  by  $(\pi^-, K^0)$  were evaluated in Ref. [16] giving a sizable contribution to the cross section. One of the technical findings of Ref. [16] is that the diagram of Fig. 2b canceled exactly the off-shell part of the meson meson amplitude in Fig 2a, which therefore requires to be evaluated with the meson meson amplitude written on shell. We should also note that the equivalent diagram of Fig. 1 in the case of the  $\pi^-p \rightarrow K^0\pi\Sigma$  reaction is strongly reduced since the emission of a  $K^0$  requires an intermediate hyperon ( $\Lambda, \Sigma$ ) state very far off shell. This is not the case in the present reaction where the intermediate proton is only moderately off shell.

The amplitude for the Feynman diagram of Fig. 2c is

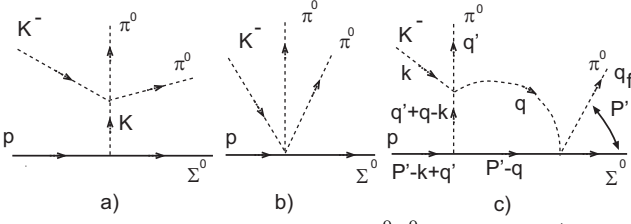


FIG. 2: Diagrams for the  $K^- p \rightarrow \pi^0 \pi^0 \Sigma$  reaction: a) K-pole term; b) MMMBB diagram - canceled by the off-shell part of a) diagram; c) one loop contribution.

given by

$$\begin{aligned}
 -it &= \int \frac{d^4 q}{(2\pi)^4} (-it_{K^- m \rightarrow \pi^0 m'}) \times \\
 &\frac{i}{(q + q' - k)^2 - M_m^2 + i\varepsilon} \frac{i}{q^2 - M_{m'}^2 + i\varepsilon} \frac{M_B}{E_B(q)} \times \\
 &\frac{i}{P'^0 - q^0 - E_B(q) + i\varepsilon} \mathcal{C}_{pBm'} \vec{\sigma}(\vec{q}' + \vec{q} - \vec{k}) (-it_{m'B \rightarrow \pi^0 \Sigma^0}), \quad (1)
 \end{aligned}$$

where  $t_{K^- m \rightarrow \pi^0 m'}$  refers to the meson meson amplitude, which we take from the lowest order chiral lagrangian [17], the  $t_{m'B \rightarrow \pi^0 \Sigma^0}$  are the meson baryon amplitudes taken from the model of Ref. [4], and the coefficients  $\mathcal{C}_{pBm'}$  are obtained from the  $D, F$  terms of the meson baryon lagrangian [18, 19] at lowest order. We take  $D + F = 1.26$  and  $D - F = 0.33$ . There are the following eight meson meson baryon ( $mm'B$ ) intermediate states:  $K^+ \pi^0 \Sigma^0$ ,  $K^+ \pi^0 \Lambda$ ,  $\pi^0 K^- p$ ,  $K^0 \pi^- \Sigma^+$ ,  $\pi^+ \bar{K}^0 n$ ,  $K^+ \eta \Sigma^0$ ,  $K^+ \eta \Lambda$ ,  $\eta K^- p$ . We note that the  $t_{K^- m \rightarrow \pi^0 m'}$  amplitude is largely dominated by the s-wave and that the linear terms in  $\vec{q}$  are further reduced in the loop due to the s-wave character of the  $t_{m'B \rightarrow \pi^0 \Sigma^0}$  amplitude. Hence, one

can factorize the on shell  $t_{K^- m \rightarrow \pi^0 m'}$  amplitude outside the integral in Eq. (1) and perform the  $q^0$  integration analytically. The  $t_{m'B \rightarrow \pi^0 \Sigma^0}$  amplitude depends on the  $(\pi^0 \Sigma^0)$  invariant mass,  $M_I^2 = (q_f + p_\Sigma)^2$ , and also factorizes outside the integral.

Altogether the amplitude for the process  $K^- p \rightarrow \pi^0 \pi^0 \Sigma^0$ , considering the diagram of Fig. 1 with a pseudovector  $\pi NN$  coupling (and keeping up to  $1/M_N$  terms) and those of Figs. 2a and 2c, is given by:

$$-it_{K^- p \rightarrow \pi^0 \pi^0 \Sigma^0} = -it^{(N\text{-pole})} - it^{(K\text{-pole})} - it^{(\text{loop})}, \quad (2)$$

with

$$\begin{aligned}
 -it^{(N\text{-pole})} &= -\frac{D+F}{2f} \vec{\sigma} \left[ \vec{q}' (1 + \frac{q'^0}{2M_N}) + \frac{q'^0}{M_N} \vec{k} \right] \times \\
 &\frac{M_N}{E_N(\vec{k} + \vec{q}') E_N(\vec{k}) - q'^0 - E_N(\vec{k} + \vec{q}')} t_{K^- p \rightarrow \pi^0 \Sigma^0} \quad (3)
 \end{aligned}$$

$$\begin{aligned}
 -it^{(K\text{-pole})} &= -\frac{1}{4f^2} (2M_\pi^2 + 2q'q_f) \frac{1}{(k - q' - q_f)^2 - M_K^2} \times \\
 &\frac{D-F}{2f} \vec{\sigma}(\vec{k} - \vec{q}' - \vec{q}_f), \quad (4)
 \end{aligned}$$

$$\begin{aligned}
 -it^{(\text{loop})} &= \sum_{j=1}^8 t_{K^- m \rightarrow \pi^0 m'}^{(j)} \mathcal{C}_{pBm'}^{(j)} \vec{\sigma}(\vec{k} - \vec{q}') t_{m'B \rightarrow \pi^0 \Sigma^0}^{(j)} \\
 &\times I(k, q', M_I, M_m^j, M_{m'}^j, M_B^j), \quad (5)
 \end{aligned}$$

where  $I(k, q', M_I, M_m^j, M_{m'}^j, M_B^j)$  is the result of the  $q^0$  integral in Eq. (1), which in the reference frame where  $\vec{P}' = 0$  (see Fig. 2c) is given by:

$$\begin{aligned}
 I(k, q', M_I, M_m, M_{m'}, M_B) &= \int \frac{d^3 q}{(2\pi)^3} \frac{1}{2\omega\omega'} \frac{M_B}{E_B(q)} [(\omega + \omega')^2 + (\omega + \omega')(E_B(q) - P'^0) + \omega(k^0 - q'^0)] \left[ 1 + \frac{\vec{q}(\vec{q}' - \vec{k})}{(\vec{q}' - \vec{k})^2} \right] \\
 &\times \frac{1}{P'^0 - k^0 + q'^0 - \omega - E_B(q) + i\varepsilon} \frac{1}{P'^0 - \omega' - E_B(q) + i\varepsilon} \frac{1}{\omega' + q'^0 - k^0 + \omega + i\varepsilon} \frac{1}{k^0 - q'^0 + \omega + \omega' - i\varepsilon}, \quad (6)
 \end{aligned}$$

with  $\omega = \sqrt{(M_m)^2 + (\vec{q} + \vec{q}' - \vec{k})^2}$  and  $\omega' = \sqrt{(M_{m'})^2 + \vec{q}^2}$ . The coefficients  $\mathcal{C}_{pBm'}$  and the meson meson amplitudes  $t_{K^- m \rightarrow \pi^0 m'}$  for the allowed ( $mm'B$ ) channels are displayed in Table I.

The indistinguishability of the two emitted pions requires the implementation of symmetrization. This is

achieved by summing two amplitudes evaluated with the two pion momenta exchanged,  $q_f \leftrightarrow q'$ , except for the diagram of Fig. 2a which is already symmetrized. In addition, a factor of 1/2 for indistinguishable particles is also included in the total cross section.

Our calculations show that the process is largely dominated by the nucleon pole term shown in Fig. 1. As a consequence, the  $\Lambda(1405)$  thus obtained comes mainly from the  $K^- p \rightarrow \pi^0 \Sigma^0$  amplitude which, as mentioned

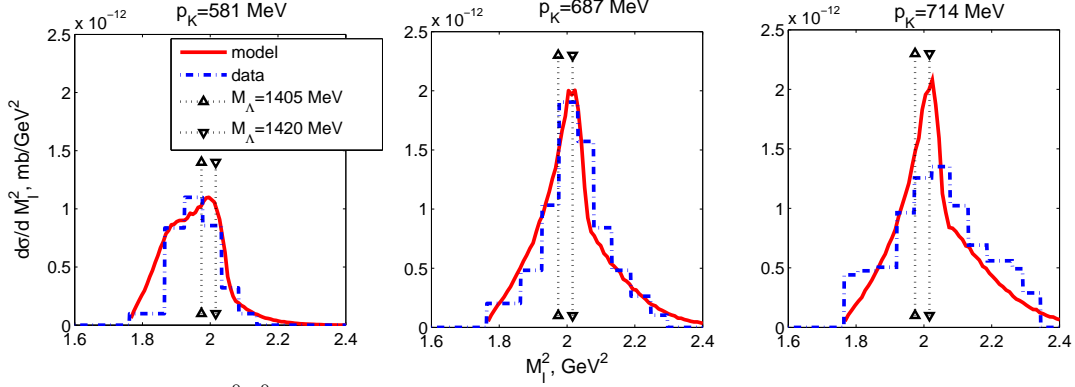


FIG. 3: The  $(\pi^0 \Sigma^0)$  invariant mass distribution for three different initial kaon momenta.

TABLE I: The  $t_{K^- m \rightarrow \pi^0 m'}$  amplitudes and  $C_{pBm'}$  coefficients for the allowed  $(mm'B)$  channels (see Eq. 5). Here  $q_{mB}^0 = \frac{M_I^2 + M_m^2 - M_B^2}{2M_I}$ .

$m$	$m'$	$B$	$t$	$C$
$K^+$	$\pi^0$	$\Sigma^0$	$-\frac{1}{4f^2} (2M_\pi^2 + 2q^0 q_{\pi\Sigma}^0)$	$\frac{D-F}{2f}$
$K^+$	$\pi^0$	$\Lambda$	$-\frac{1}{4f^2} (2M_\pi^2 + 2q^0 q_{\pi\Lambda}^0)$	$-\frac{2}{\sqrt{3}} \frac{D-F}{2f} + \frac{1}{\sqrt{3}} \frac{D+F}{2f}$
$\pi^0$	$K^-$	$p$	$-\frac{1}{4f^2} (2M_K^2 - 2k^0 q_{Kp}^0)$	$\frac{D+F}{2f}$
$K^0$	$\pi^-$	$\Sigma^+$	$-\frac{\sqrt{2}}{2f^2} (k^0 q_{\pi\Sigma}^0 - k^0 q^0 + \vec{k} \vec{q})$	$\sqrt{2} \frac{D-F}{2f}$
$\pi^+$	$\bar{K}^0$	$n$	$-\frac{\sqrt{2}}{2f^2} (M_K^2 - M_\pi^2 - q^0 q_{Kn}^0 - k^0 q^0 + \vec{k} \vec{q})$	$\sqrt{2} \frac{D+F}{2f}$
$K^+$	$\eta$	$\Sigma^0$	$-\frac{\sqrt{3}}{12f^2} (3t - \frac{8}{3} M_K^2 - \frac{1}{3} M_\pi^2 - M_\eta^2),$ where $t = M_\pi^2 + M_\eta^2 + 2q^0 q_{\eta\Sigma}^0$	$\frac{D-F}{2f}$
$K^+$	$\eta$	$\Lambda$	$-\frac{\sqrt{3}}{12f^2} (3t - \frac{8}{3} M_K^2 - \frac{1}{3} M_\pi^2 - M_\eta^2),$ where $t = M_\pi^2 + M_\eta^2 + 2q^0 q_{\eta\Lambda}^0$	$-\frac{2}{\sqrt{3}} \frac{D+F}{2f} + \frac{1}{\sqrt{3}} \frac{D-F}{2f}$
$\eta$	$K^-$	$p$	$-\frac{\sqrt{3}}{12f^2} (3t - \frac{8}{3} M_K^2 - \frac{1}{3} M_\pi^2 - M_\eta^2),$ where $t = 2M_K^2 - 2k^0 q_{Kp}^0$	$\frac{1}{\sqrt{3}} \frac{D+F}{2f} - \frac{2}{\sqrt{3}} \frac{D-F}{2f}$

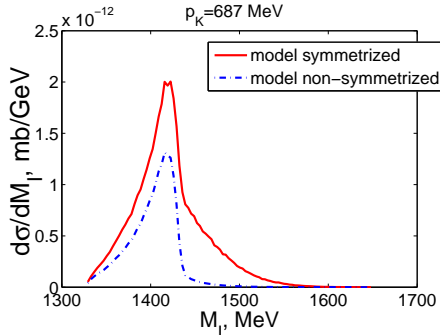


FIG. 4: Theoretical  $(\pi^0 \Sigma^0)$  invariant mass distribution for an initial kaon lab momenta of 687 MeV. The non-symmetrized distribution also contains the factor  $1/2$  in the cross section.

above, gives the largest possible weight to the second (narrower) state.

In Fig. 3 our results for the invariant mass distribution for three different energies of the incoming  $K^-$  are compared to the experimental data. Symmetrization of the amplitudes produces a sizable amount of background. At a kaon laboratory momentum of  $p_K = 581$  MeV/c this background distorts the  $\Lambda(1405)$  shape producing cross section in the lower part of  $M_I$ , while at  $p_K = 714$

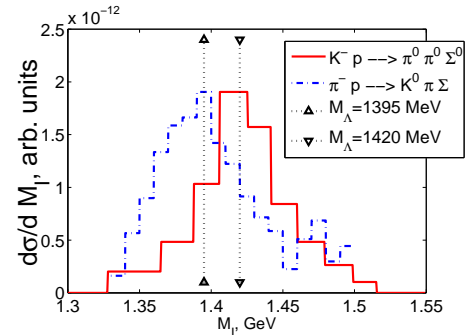


FIG. 5: Two experimental shapes of  $\Lambda(1405)$  resonance. See text for more details.

MeV/c the strength of this background is shifted toward the higher  $M_I$  region. An ideal situation is found for momenta around 687 MeV/c, where the background sits below the  $\Lambda(1405)$  peak distorting its shape minimally. The peak of the resonance shows up at  $M_I^2 = 2.02$   $\text{GeV}^2$  which corresponds to  $M_I = 1420$  MeV, larger than the nominal  $\Lambda(1405)$ , and in agreement with the predictions of Ref. [8] for the location of the peak when the process is dominated by the  $t_{\bar{K}N \rightarrow \pi\Sigma}$  amplitude. The apparent width from experiment is about 40 – 45 MeV, but a precise determination would require to remove the background mostly coming from the “wrong”  $\pi^0 \Sigma^0$  cou-

ples due to the indistinguishability of the two pions. A theoretical analysis permits extracting the pure resonant part by not symmetrizing the amplitude. This is plotted in Fig. 4 as a function of  $M_I$ . The width of the resonant part is  $\Gamma = 38$  MeV, which is smaller than the nominal  $\Lambda(1405)$  width of  $50 \pm 2$  MeV [20], obtained from the average of several experiments, and much narrower than the apparent width of about 60 MeV that one sees in the  $\pi^- p \rightarrow K^0 \pi \Sigma$  experiment [21], which also produces a distribution peaked at 1395 MeV. In order to illustrate the difference between the  $\Lambda(1405)$  resonance seen in this latter reaction and in the present one, the two experimental distributions are compared in Fig. 5. We recall that the shape of the  $\Lambda(1405)$  in the  $\pi^- p \rightarrow K^0 \pi \Sigma$  reaction was shown in Ref. [16] to be largely built from the  $\pi \Sigma \rightarrow \pi \Sigma$  amplitude, which is dominated by the wider lower energy state.

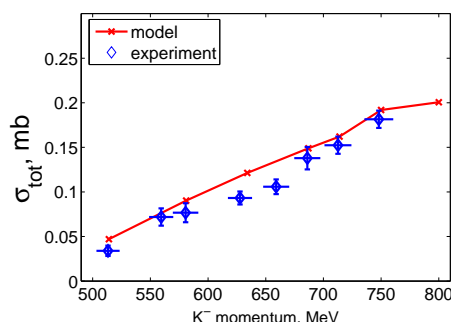


FIG. 6: Total cross section for the reaction  $K^- p \rightarrow \pi^0 \pi^0 \Sigma^0$ . Experimental data are taken from Ref. [15].

The invariant mass distributions shown here are not normalized, as in experiment. But we can also compare

our absolute values of the total cross sections with those in Ref. [15]. As shown in Fig. 6, our results are in excellent agreement with the data, in particular for the three kaon momentum values whose corresponding invariant mass distributions have been displayed in Fig. 3.

In summary, we have shown, by means of a realistic model, that the  $K^- p \rightarrow \pi^0 \pi^0 \Sigma^0$  reaction is particularly suited to study the features of the second pole of the  $\Lambda(1405)$  resonance, since it is largely dominated by a mechanism in which a  $\pi^0$  is emitted prior to the  $K^- p \rightarrow \pi^0 \Sigma^0$  amplitude, which is the one giving the largest weight to the second narrower state at higher energy. Our model has proved to be accurate in reproducing both the invariant mass distributions and integrated cross sections seen in a recent experiment [15]. The study of the present reaction, complementary to the one of Ref. [16] for the  $\pi^- p \rightarrow K^0 \pi \Sigma$  reaction, has shown that the quite different shapes of the  $\Lambda(1405)$  resonance seen in these experiments can be interpreted in favour of the existence of two poles with the corresponding states having the characteristics predicted by the chiral theoretical calculations. Besides demonstrating once more the great predictive power of the chiral unitary theories, this combined study of the two reactions gives the first clear evidence of the two-pole nature of the  $\Lambda(1405)$ .

**Acknowledgments:** This work is partly supported by DGICYT contracts BFM2002-01868, BFM2003-00856, the Generalitat de Catalunya contract SGR2001-64, and the E.U. EURIDICE network contract HPRN-CT-2002-00311. This research is part of the EU Integrated Infrastructure Initiative Hadron Physics Project under contract number RII3-CT-2004-506078.

- 
- [1] M. Jones, R. H. Dalitz and R. R. Horgan, Nucl. Phys. B **129** (1977) 45.
  - [2] N. Kaiser, P. B. Siegel and W. Weise, Phys. Lett. B **362** (1995) 23
  - [3] N. Kaiser, T. Waas and W. Weise, Nucl. Phys. A **612** (1997) 297 [arXiv:hep-ph/9607459].
  - [4] E. Oset and A. Ramos, Nucl. Phys. A **635** (1998) 99 [arXiv:nucl-th/9711022].
  - [5] J. A. Oller and U. G. Meissner, Phys. Lett. B **500** (2001) 263 [arXiv:hep-ph/0011146].
  - [6] D. Jido, A. Hosaka, J. C. Nacher, E. Oset and A. Ramos, Phys. Rev. C **66** (2002) 025203 [arXiv:hep-ph/0203248].
  - [7] C. Garcia-Recio, J. Nieves, E. Ruiz Arriola and M. J. Vicente Vacas, Phys. Rev. D **67** (2003) 076009 [arXiv:hep-ph/0210311].
  - [8] D. Jido, J. A. Oller, E. Oset, A. Ramos and U. G. Meissner, Nucl. Phys. A **725** (2003) 181 [arXiv:nucl-th/0303062].
  - [9] C. Garcia-Recio, M. F. M. Lutz and J. Nieves, Phys. Lett. B **582** (2004) 49 [arXiv:nucl-th/0305100].
  - [10] T. Hyodo, S. I. Nam, D. Jido and A. Hosaka, Phys. Rev. C **68** (2003) 018201 [arXiv:nucl-th/0212026].
  - [11] S. I. Nam, H. C. Kim, T. Hyodo, D. Jido and A. Hosaka, arXiv:hep-ph/0309017.
  - [12] J. C. Nacher, E. Oset, H. Toki and A. Ramos, Phys. Lett. B **461** (1999) 299 [arXiv:nucl-th/9902071].
  - [13] T. Hyodo, A. Hosaka, M. J. Vicente Vacas and E. Oset, Phys. Lett. B **593** (2004) 75 [arXiv:nucl-th/0401051].
  - [14] T. Nakano, private communication.
  - [15] S. Prakhov *et al.* [Crystall Ball Collaboration], Phys. Rev. C **70** (2004) 034605.
  - [16] T. Hyodo, A. Hosaka, E. Oset, A. Ramos and M. J. Vicente Vacas, Phys. Rev. C **68** (2003) 065203 [arXiv:nucl-th/0307005].
  - [17] J. Gasser and H. Leutwyler, Nucl. Phys. **B250** (1985) 465, 517, 539.
  - [18] U. G. Meissner, Rep. Prog. Phys. **56** (1993) 903; V. Bernard, N. Kaiser and U. G. Meissner, Int. J. Mod. Phys. E4 (1995) 193.
  - [19] G. Ecker, Prog. Part. Nucl. Phys. **35** (1995) 1.
  - [20] K. Hagiwara *et al.* [Particle Data Group], Phys. Rev. D **66**, 010001 (2002).
  - [21] D. W. Thomas, A. Engler, H. E. Fisk, and R. W. Kraemer, Nucl. Phys. B **56**, 15 (1973).